

Frictional mechanics of knots

May 2023

Ulrich Leuthäusser

ulrich.leuthaeusser@aon.at

Abstract

For some important knots closed-form solutions are presented for the holding forces which are needed to keep a knot in equilibrium for given pulling forces. If the holding forces become zero for finite pulling forces, the knot is self-locking and is called stable. This is only possible when first, the friction coefficient exceeds a critical value and second, when there is additional pressure on some knot segments sandwiched by surrounding knot segments. The number of these segments depends on the topology of the knot and is characteristic for it. The other important parameter is the total curvature of the knot. In this way, the complete frictional contact inside the knot is taken into account. The presented model can explain the available experiments.

Key words

Self-locking knots, contact mechanics, contact angle, stability, Euler-Eytelwein equation

Acknowledgements

The author thanks Ira Leuthäusser for helpful discussions and critical reading of the manuscript.

Declaration of conflicting interests

The author declares no potential conflicts of interest with respect to the research, authorship and/or publication of this article.

Funding

The author received no financial support for the research, authorship and/or publication of this article.

1. Introduction

Because of their eminent importance and ubiquity, knots have been and are being intensively investigated from a wide variety of aspects.

First, there is an abstract mathematical approach known as knot theory [1]. It ignores the physical properties of knots and investigates their topological properties studying mainly the equivalence of one-dimensional closed curves in space. Nevertheless, it has applications including chemistry, biological and polymer physics, statistical mechanics and quantum field theory. Next, there is a more physics-driven approach, the so-called physical knot theory which [2] has received less attention than its abstract cousin and to which this paper belongs. In physical knot theory, knots are not treated as abstract, closed curves. Instead, a knot is mostly considered as a connection between two ends of a rope in order to investigate the tension and friction forces within the knot. Questions about its breaking strength and its stability can be answered in this way. Numerous important applications range from surgical knots to knots for sailing and mountaineering. Finally, there are some applied, non-mathematical papers that are valuable from a practical point of view [3].

In 1976, Bayman [4] asked, under which circumstances a hitch locks itself. That means, when it will withstand a pulling force without an opposite holding force. Using classical mechanics, he gave a criterion for this self-locking phenomenon. Maddocks and Keller [5] extended Bayman's approach to knots and investigated the forces occurring in the knot in more detail. They got some testable results for simple knots or part of simple knots. However, experiments [6] do not completely agree with their predictions. In a recent paper [7], elements of mathematical knot theory have been combined with mechanics in order to get some topological criteria for the holding abilities of knots. In addition, measurements of the pulling force necessary to untie a knot for a given holding force were presented for several important knots.

This work provides an analysis of the forces that arise in a knot when external pulling forces are applied. The holding forces necessary to keep the knot in equilibrium are calculated. For many of the here discussed knots, there is a critical static friction coefficient μ_c at which the knot behavior changes qualitatively. For friction coefficients $\mu \geq \mu_c$ the holding force becomes zero regardless of the strength of the pulling force. In this paper, a knot is called stable if it shows this behavior. For unstable knots there is no such μ_c , that is, a holding force is always necessary to avoid that the knot slips. This stability has to be distinguished from structural stability, i.e. a strong deformation of the knot, a geometric change or even capsizing of the knot. Structural stability is a necessary condition for the above stability. The methods used here are classical equilibrium mechanics with Coulomb friction just at the verge of impending motion. As in Refs. [4] and [5], a perfectly flexible and inextensible rope material without any bending and torsion forces is assumed. Bending rigidity can be taken into account using an additional force term proportional to the bending angle. The bulky results, however, show no qualitative differences and are omitted.

The paper is organized as follows. In the next section, the necessary preliminaries for the subsequent calculations are made. To treat the simultaneous contact of three knot segments, it is necessary to generalize the Euler-Eytelwein equation for this case. In section 3, a general procedure for the calculation of the appearing forces in the knot is presented. It will be shown that the ratio of holding and pulling force has a common structure for all investigated knots. Next, this ratio is derived for the most important knots (square knot and its relatives, etc.) and presented as closed-form formulas together with the critical friction coefficients. The question of why the granny knot is less stable than the square knot is answered. Furthermore, a relation to directed graphs is established, showing that feedback effects are necessary for a stable node. In section 5, the discussed knots are summarized and a comparison with experimental results is carried out.

2. A generalized Euler-Eytelwein equation and a self-locking mechanism

In this section, the well-known Euler-Eytelwein equation [8] is generalized in a simple way for its application to knots. With this equation, it is possible to calculate the force F that is necessary to pull a piece of rope over a curved surface to overcome both the opposing holding force and the friction force between rope and surface. The generalization introduces an additional external force N_e acting on that piece of rope. This allows to describe the contact of three rope segments where a sandwiched rope segment is compressed by two other rope segments.

To derive this equation, consider Fig. 1 of an infinitesimal segment of a rope which in contact with another segment. μ is the friction coefficient for this contact. An infinitesimal external force dN_e acts on this segment in negative y-direction and causes an additional friction force $\mu_e dN_e$ in tangential direction.

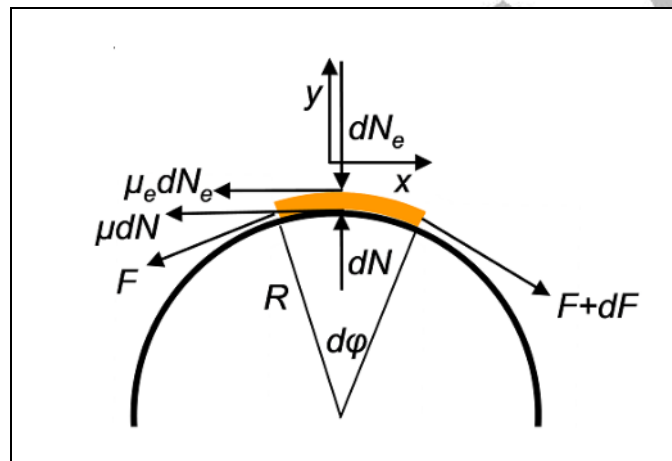


Fig.1. Free body diagram of the yellow infinitesimal rope element with an additional external normal force dN_e .

The equilibrium force equations in x and y direction are given by

$$\begin{aligned} dF &= \mu dN + \mu_e dN_e, \\ dN &= F d\varphi + dN_e. \end{aligned}$$

Replacing dN in the first equation by the second and introducing the pressure

$$n_e(\varphi) = \frac{1}{R(\varphi)} \frac{dN_e}{d\varphi}$$

with the local radius $R(\varphi)$ of the lower segment, one obtains

$$\frac{dF}{d\varphi} = \mu F + (\mu + \mu_e) R(\varphi) n_e(\varphi). \quad (1)$$

Without the external pressure $n_e(\varphi)$, the classical Euler-Eytelwein equation with an exponentially increasing $F(\varphi)$ is obtained.

A the simple solution of Eq. (1) for a constant external pressure $n_e = \frac{N_e}{R(\varphi_1 - \varphi_0)}$ for

$\varphi_0 \leq \varphi \leq \varphi_1$ is given by

$$F(\varphi) = F(0)e^{\mu\varphi} + \frac{\mu + \mu_e}{\mu} \frac{N_e}{\varphi - \varphi_0} \left[\Theta(\varphi - \varphi_1)(1 - e^{\mu(\varphi - \varphi_1)}) - \Theta(\varphi - \varphi_0)(1 - e^{\mu(\varphi - \varphi_0)}) \right], \quad (2)$$

using the unit step function $\Theta(\varphi)$. For a localized force N_e at $\varphi_0 = \varphi_1$, Eq. (2) reduces to

$$F(\varphi) = F(0)e^{\mu\varphi} + (\mu + \mu_e)N_e\Theta(\varphi - \varphi_1)e^{\mu(\varphi - \varphi_1)}, \quad (3)$$

which will be used later in the discussion of several knots. Consider a second rope segment above the first which moves with the same external force N_e in the opposite direction (now acting on both ropes). Then for $\mu = \mu_e$, a factor 4 appears instead of a factor 2 counting the number of frictional contacts induced by N_e .

The second example (see Fig. 2), as a part of an overhand knot, is a rope that, after passing over the cylinder A and reversing without friction its direction at B, presses within a certain angle segment β on itself. This interaction between different rope parts leads to self-locking where no holding force F_1 is necessary to oppose the pulling force F_0 .

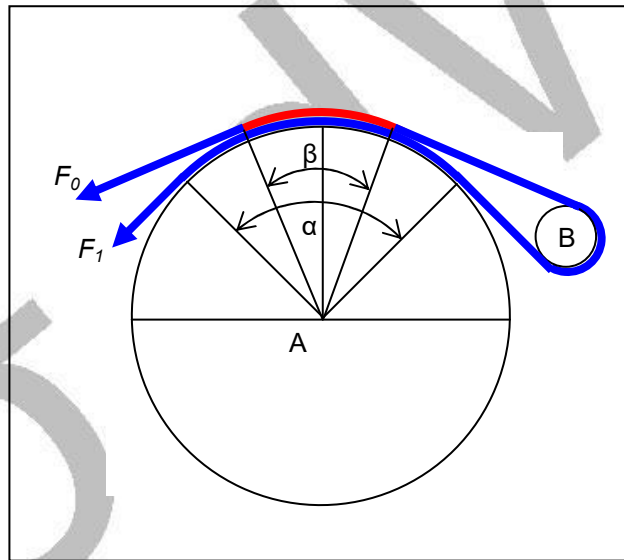


Fig. 2. A rope in contact with a cylinder A within sector α . The rope is pressed by itself onto the cylinder A within sector β after it is frictionless reversed at B.

To keep it simple, a symmetric arrangement with equal friction coefficients $\mu = \mu_e$ is chosen (see Fig. 2). The additional pressure from the upper piece of the rope is given by

$$n_e(\varphi) = \frac{1}{R} F_0 e^{\mu \left(\frac{1}{2}(\alpha + \beta) - \varphi \right)} \quad (4)$$

with φ in the interval $\frac{1}{2}(\alpha - \beta) < \varphi < \frac{1}{2}(\alpha + \beta)$. The solution of Eq. (1) becomes

$$F_1 = F_0 e^{-\mu\Phi} \left(1 - 2 \sinh(\mu\beta) e^{\mu\frac{\Phi}{2}} \right), \quad (5)$$

where the total contact angle $\Phi = \alpha + \beta$ has been introduced. Because a pushing (negative) F_1 is not possible, Eq. (5) is only valid for $F_1 \geq 0$.

Without a reversal of motion at B, the rope wraps around the cylinder (see Fig. 2), so that both parts of the rope move together in the same direction. In this case, Eq. (5) has to be modified, with $\Phi = \alpha$ and with the replacement $\beta \rightarrow \beta/2$.

Eq. (5) has the typical structure which will later also appear for knots. The first term $e^{-\mu\Phi}$ is the solution of the usual Euler-Eytelwein equation containing the friction contributions from the contact angles α and β coming solely from the rope tensions from a single contact. The second term describes the effect of the additional pressure on the sandwiched part of the rope in the β -segment what makes self-locking possible. For every $\beta > 0$, there is always a zero of Eq. 5 for a friction coefficient μ_c which has to be calculated numerically. The transformation $\mu \rightarrow -\mu$ swaps F_0 and F_1 , the zero disappears and stability is lost. As expected, a holding force is always necessary when the lower part of the rope is pulled.

It is important to note that Eq. (1) in this form is only valid in a plane. If the curved surface is a space curve, $d\varphi$ has to be replaced by $\kappa(s)ds$ with ds as the infinitesimal arc length and $\kappa(s)$ as the curvature which is a function of s . One gets

$$\frac{dF}{ds} = \mu\kappa(s)F + (\mu + \mu_e)n_e(s). \quad (6)$$

Integrating Eq. (6), the angle φ in the Euler-Eytelwein equation becomes the so-called total curvature [9]

$$\varphi \rightarrow \Phi = \int_0^L \kappa(s)ds \quad (7)$$

which is called contact angle here. L is the complete arc length of the contact and Φ can therefore be expressed by the average curvature $\langle \kappa \rangle = \Phi/L$.

An example of a space curve which is needed in section 4 is a helix around a circular cylinder with radius R . A helix has constant curvature, so that Eq. (6) can easily be integrated. For $n_e = 0$ one gets

$$F = F_0 \exp\left(\mu \frac{R}{R^2 + (h/2\pi)^2} L\right) = F_0 \exp\left(\mu \frac{R}{\sqrt{R^2 + (h/2\pi)^2}} \varphi\right).$$

h is the height of one complete helix turn by 2π , called pitch. It is interesting to note that for a fixed angle φ (as the angular coordinate of the cylindrical coordinates it is equivalent to φ of the planar case), the friction vanishes for large h . Although the contact length L increases with h , it is overcompensated by a diminishing curvature. This is the reason why two identical knots, the one that is tied stronger and therefore smaller in size, have a larger holding force. For the estimation of Φ it is sometimes useful to divide the space curve piecewise into a polygon lying in different oriented planes. The total curvature is then the sum of the angles between subsequent line segments using the dot product.

3. The analysis of a knot

In this section, a general procedure for the calculation of the forces in a knot is presented using the results of the last section.

First the knot is decomposed into suitable segments which are determined by their mutual contact points (see Fig. 3). For example, the segment $\overline{34}$ in Fig. 3 is in contact with the segment $\overline{2'3'}$ of the other strand, but touches also segment $\overline{01}$ of the same strand. But $\overline{2'3'}$ is only in contact with $\overline{34}$. The endpoints of these segments are labeled and the forces F_n together with their directions are assigned to them. One starts with the known pulling force F_0 as input and ends at the endpoint of the knot with the holding force F_n as output. Superfluous node points do not change the analysis.

Symmetry operations like reflections and rotations which leave the knot invariant reduce the number of unknown forces. So, for example, for the highly symmetric square knot of Fig. 3, the number of unknown forces is reduced by a factor 2. The rest has to be determined by force equilibrium conditions.

Choosing an appropriate coordinate system makes it sometimes possible to set up simple equilibrium equations for certain force components. For example, the forces in z direction in the white y'z-plane of Fig. 3 yield the normal forces on the compressed rope segments, as will be shown later.

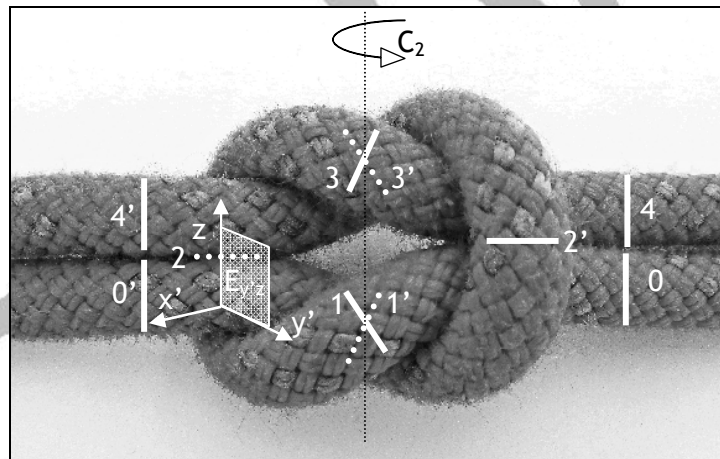


Fig. 3. Picture of a square knot. The division into 4 segments is shown for both strands of the knot (the segments of the left strand are indicated by primed numbers). The segment boundaries that are not visible because they are covered by knot segments above them are drawn with dots. Because of the rotational invariance around the C_2 axis, the segmentation of the 2 strands is identical. The segments $\overline{12}$ and $\overline{2'3'}$ lie almost entirely in the plane $E_{y'z}$. The $x'y'z$ coordinate system is rotated around z with the original y -axis lying in the drawing plane.

The unknown forces F_1, F_2, \dots, F_n and the given pulling force F_0 form a system of linear force balance equations

$$AF = F_0 b \tag{8}$$

with the $n \times n$ matrix

$$A = \begin{pmatrix} e^{\mu\phi_1} & a_{12} & \cdots & a_{1n} \\ -1 & e^{\mu\phi_2} & \cdots & a_{2n} \\ \vdots & \ddots & \ddots & \vdots \\ a_{n1} & \cdots & -1 & e^{\mu\phi_n} \end{pmatrix}$$

The special form of A with only minus ones in the subdiagonal and with diagonal elements $a_{ii} = e^{\mu\phi_i}$ comes from the Euler-Eytelwein friction contributions between consecutive forces F_i and F_{i+1} . b is a known vector with values resembling the matrix elements of A . In its simplest form, it is given by $(1, 0, 0, \dots, 0)$. b is multiplied with the known input force F_0 . Interested in the holding force F_n , application of Cramer's formula yields

$$T(\mu) = \frac{F_n}{F_0} = \frac{\det(A_n)}{\det(A)}. \quad (9)$$

A_n is the matrix A with its n^{th} column replaced by the vector $F_0 b$. T is called transfer function because only part of the input pulling force F_0 is transferred through the knot leading to a smaller output holding force F_n . The total friction force in the knot is given by $F_{fr} = F_0(1 - T)$. For $a_{ij} = 0$ except a_{ii} and $a_{i-1,i}$, the transfer function is $T(\mu) = e^{-\mu\Phi}$ with $\Phi = \sum_i \phi_i$ as the total contact angle. $e^{-\mu\Phi}$ takes into account only the contact between the complete rope strand and its touching counterpart or with itself. It is the trivial solution for T without additional compression forces. In other words, if there are only contacts between two rope segments, the Euler-Eytelwein equation is sufficient to calculate the forces at the ends of the segments.

The general solution of Eq. (9) can always be written as

$$T(\mu) = e^{-\mu\Phi} \frac{1 - G(\mu)}{1 + H(\mu)} \quad (10)$$

with $1 + H(\mu) = e^{-\mu\Phi} \det(A)$ and $1 - G(\mu) = \det(A_n)$.

Because T can never be larger than one, G and H are always nonnegative. The condition for self-locking is the existence of a critical μ_c that satisfies

$$1 - G(\mu_c) \equiv 0. \quad (11)$$

The reversal of input and output force leading to a reversal of the impending motion is described by the transformation $\mu \rightarrow -\mu$. If the knot symmetry leaves the physics unchanged (that is, a symmetry operation can restore the same knot including the forces acting on it), one gets

$$T(\mu)T(-\mu) = 1, \quad (12)$$

from which $H(\mu) = -G(-\mu)$ follows. Therefore

$$T(\mu) = e^{-\mu\Phi} \frac{1+H(-\mu)}{1+H(\mu)}. \quad (13)$$

Thus, the self-locking condition of Eq. (11) is equivalent to an eigenvalue of $A(-\mu)$ equal to zero.

Eq. (10) for T is reminiscent to Mason's formula [10] from signal flow analysis which allows a graphical representation of the knot as a directed graph (an example is given in section 4). $e^{-\mu\Phi}$ is the contribution of the forward path $F_0 \rightarrow F_1 \rightarrow \dots \rightarrow F_n$ touching all nodes. In signal flow analysis, G is interpreted as gains from additional forward paths and H describes feedback effects. To obtain self-locking, at least one additional forward path is necessary.

4. The square knot and related knots

The square knot is a simple, symmetric knot that many of us use every day. Because of some controversy about the comparison with its close relative, the granny knot, the square knot is of particular interest.

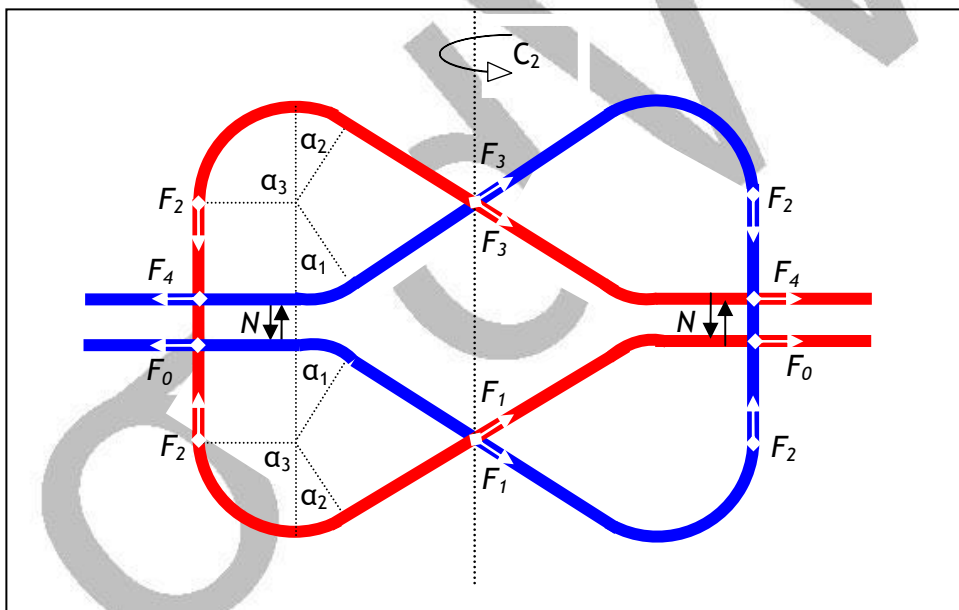


Fig. 4. The square knot with the forces F_n at positions n . For example, at the ends of segment $\overline{01}$ the forces F_0 and F_1 are present. This rope segment $\overline{01}$ is in contact with segment $\overline{12}$ with an additional force N on it.

The square knot is indistinguishable from its initial position after a rotation about the axis C_2 (i.e. rotated by π). This rotational symmetry reduces the number of forces and contact angles α_i inside the knot.

The α_i have been defined by Eq. (7) as

$$\alpha_i = \int_0^{\text{arclength}_i} \kappa(s) ds.$$

In Fig. 4 the projections of these angles into the drawing plane are shown. Starting from the pulling force F_0 , the normal force N acts before the curved arc between 0 and 1 begins. Therefore by application of Eq. (3) one finds

$$F_0 = F_1 e^{\mu\alpha_1} + 2\mu N. \quad (14)$$

The rope segment $\overline{34}$ moves in the opposite direction of segment $\overline{01}$, thus

$$F_3 = (F_4 + 2\mu N) e^{\mu\alpha_1}. \quad (15)$$

For the segments $\overline{12}$ and $\overline{23}$, where no additional normal forces are present, one has

$$\frac{F_2}{F_1} = \frac{F_3}{F_2} = e^{-\mu(\alpha_2 + \alpha_3)}. \quad (16)$$

N lies in the plane E_{yz} of Fig. 3 in z direction. In equilibrium, the forces must fulfill

$$N = F_2 \sin \alpha_3 + F_1 \sin \alpha'_1 - F_1 \sin \alpha'_2. \quad (17)$$

Because of the knot symmetry, the angles α'_1 and α'_2 as projections of α_1 and α_2 into the plane E_{yz} are equal. The angle α_3 completely lies in E_{yz} and given by $\pi/2$. Thus

$$N = F_2. \quad (18)$$

Inserting this result into Eqs. (14) and (15) one obtains together with Eqs. (16)

$$T = \frac{F_4}{F_0} = e^{-\mu\Phi_s} \frac{1 - 2\mu e^{\frac{\mu\Phi_s}{2}}}{1 + 2\mu e^{-\frac{\mu\Phi_s}{2}}}, \quad (19)$$

where the total contact angle

$$\Phi_s = 2 \left(\alpha_1 + \alpha_2 + \frac{\pi}{2} \right) \quad (20)$$

has been introduced to eliminate the contact angles $\alpha_1 + \alpha_2$. T is only a function of Φ_s and μ and it satisfies the symmetry relation (12). If the normal force N is neglected, one obtains

$T = e^{-\mu\Phi_s}$ where only the total curvature enters for the resulting holding force. Self-locking

occurs at μ_c as a solution of the equation $1 = 2\mu e^{\frac{\mu\Phi_s}{2}}$. This result has been obtained by

Maddocks and Keller [5] for $\Phi_s = 2\pi$.

For an input force $F_0 = 0$, all other subsequent forces are zero and therefore also the total frictional force. In this simple linear model there are no remnant friction forces which hold the force-free knot together, i.e. it disintegrates as soon as the external pulling-forces are absent. Actually, these remnant internal forces are small. This can easily be checked. For example, a tightened square knot that is shaken loosens.

The complicated calculation of Φ_s can be done only numerically. Because Φ_s depends on how the knot is tightened, it is not an invariant of the knot. Thus, an estimate should be

sufficient here. The approach uses the numerically determined lengths $L_{ot} = 10.1$ and $L_{ct} = 16.37$ in units of the rope radius R of the open and the closed trefoil knot [11, 12]. Because the open trefoil knot can be assembled from the square knot and a helix segment with pitch $8 \cdot R$ (see Fig.5), the following equation

$$\Phi_s + \frac{\pi}{\sqrt{1 + \left(\frac{8}{2\pi}\right)^2}} = \Phi_{ot} = \langle \kappa_{ot} \rangle L_{ot} = \frac{\Phi_{ct} - \Phi_{ot}}{L_{ct} - L_{ot}} L_{ot}$$

is obtained, where it was assumed that the mean curvatures of the open and closed trefoil knot are equal. The difference of the two contact angles is $\Phi_{ct} - \Phi_{ot} \cong 2\pi$, so that the result for the square knot is $\Phi_s = 2.60\pi$. A very tight square knot has a maximum $\Phi_s^{\max} = 3\pi$.

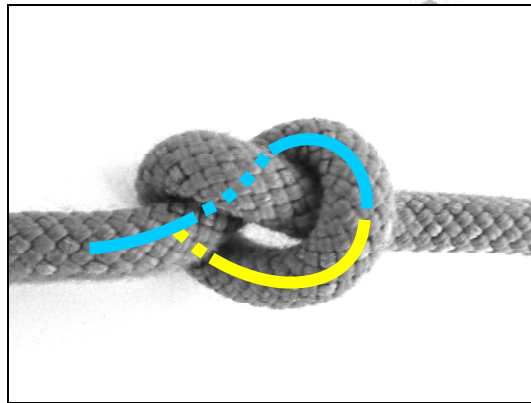


Fig.5. Picture of the open trefoil knot. It can be assembled by the yellow segment, the blue segment and a segment identical to the blue obtained by rotation about C_2 (not shown).

Some new insights can be gained by the representation of the knot using signal-flow analysis [10]. In Fig. 6 the signal-flow graph of the square knot is shown. The set of linear equations is equivalent to a directed graph which shows the dependency between the forces in a transparent way. F_0 is the input node and F_4 the output node. Besides the multiplicative gains a, b, c, d between successive nodes, the interesting parts are the feedback gain $b \cdot f$ and the feedforward gain g which are responsible for self-locking. Mason's gain formula as the main result of signal-flow graph analysis immediately gives Eq.(19).

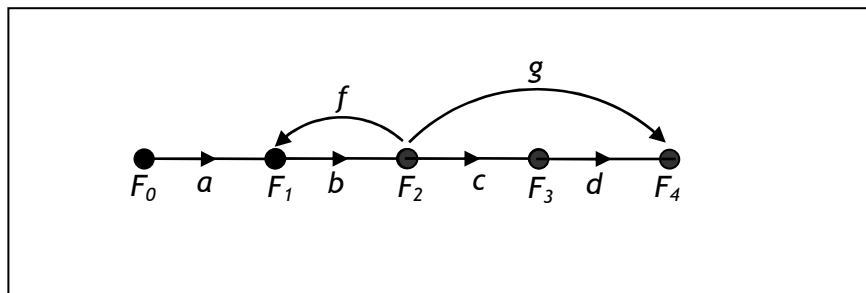


Fig. 6. The signal flow graph of the square knot. The coefficients which connect the nodes are given by $a = d = e^{-\mu\alpha_1}$, $b = c = e^{-\mu(\alpha_1 + \alpha_3)}$, $f = -2\mu e^{-\mu\alpha_1}$, $g = -2\mu$.

The granny knot

Like the square knot, the granny knot is invariant under a rotation about the axis C_2 . Because of that strong resemblance, the analysis of the granny knot follows the same steps as before for the square knot.

There is also a normal force N that presses the two inner rope segments together. Therefore Eq. (19) is also valid for the granny knot. However, it has to be taken into account that, because of its smaller structural stability, the granny knot needs to be tied more carefully than the square knot. Having the same T as the square knot, the granny is also a stable knot, but there is a major difference to the square knot, namely its smaller contact angle Φ_g .

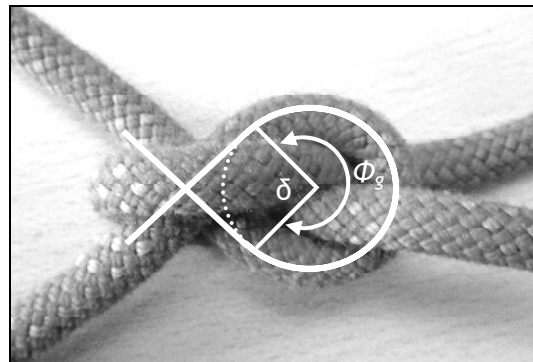


Fig. 7. Picture of the granny knot seen from above. It consists of two mutually perpendicular loops that are almost planar.

In contrast to the square knot where the rope strands form a space curve, the loops of the granny knot lie almost entirely in a plane (see Fig. 7). This immediately leads to $\Phi_g = 2\pi - \delta$.

Again, the comparison with the open trefoil knot allows to determine the contact angle Φ_g . The trefoil knot can be divided into two circular sectors each representing the contact angle Φ_g so that

$$\Phi_g = \frac{1}{2} \langle \kappa_{ot} \rangle L_{ot} = 1.61\pi.$$

A very tight granny knot has a maximum $\Phi_g^{\max} = 2\pi$.

The difference in the contact angles Φ_s and Φ_g significantly affects the range in which the knots are stable and secure.

This can be shown by a sensitivity analysis of the transfer function T . The starting point of the analysis is a rope with a certain $\mu > \mu_c$ which is tied to a stable square resp. granny knot.

Now small changes in the contact angle are assumed occurring for example when the input and output force change slightly their direction. What perturbation in Φ can still be accepted so that the knots remains stable? The sensitivity of T against variations of Φ is extreme in

the neighborhood of that Φ for which the knot becomes unstable, i.e. $\Phi_c(\mu) = \frac{2}{\mu} \ln\left(\frac{1}{2\mu}\right)$.

The sensitivity of T , $S_{\Phi}^T = \frac{d|T(\Phi)|}{d\Phi} \frac{1}{|T(\Phi)|}$ decays on a scale of $\frac{1}{2\mu}$. As a measure of security, the relative, barely tolerable perturbation $\delta(\Phi, \mu)$ is therefore given by

$$\delta(\Phi, \mu) = \frac{\Phi - \left(\Phi_c - \frac{1}{2\mu} \right)}{\Phi} = 1 - \frac{1}{\Phi} \left(\frac{2}{\mu} \ln \left(\frac{1}{2\mu} \right) + \frac{1}{2\mu} \right).$$

In case of the square knot, $\delta(\Phi_s = 2.6\pi, \mu = 0.3) = 38\%$ is obtained. For the granny knot, however, the corresponding result is $\delta(\Phi_g = 1.6\pi, \mu = 0.3) < -1\%$. Thus, $\mu = 0.3$ is not large enough for a secure granny knot.

The theft knot

If one swaps F_0 and F_4 of the square knot (see Fig. 4) on the right side of the node, a new configuration is created, called theft knot. The corresponding case starting from the granny knot is called grief knot. Because the two strands of the knot are not in a line, a shear movement is created.

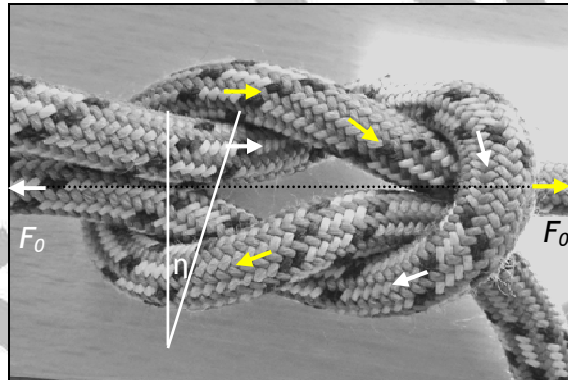


Fig. 8. Theft knot with a force couple F_0 which creates the shear angle η and with the directions of the occurring forces in both knot strands.

This movement stops for a certain shear angle η when the external torque created by the force couple F_0 becomes zero. The corresponding equilibrium condition to Eq. (17) is changed and a much smaller normal force N results. In addition, the number of compressed parts which move against each other is reduced by a factor two. As a consequence, the theft knot is unstable. Its transfer function is given by

$$T \approx e^{-\mu\Phi} \frac{1 - \mu \left(e^{\frac{\mu\Phi}{2}} - \frac{1}{2}\eta(1 + e^{\mu\Phi}) \right)}{1 + \mu \left(e^{-\frac{\mu\Phi}{2}} - \frac{1}{2}\eta(1 + e^{-\mu\Phi}) \right)} + O(\mu^2\eta). \quad (21)$$

The zero in the numerator for a critical μ disappears for small angles $\eta < 10^\circ$ (using

$\Phi = 2.6\pi$). However, the resulting η which is determined by the equilibrium condition of a zero torque is about 20° .

Clove hitch and Munter hitch

The clove hitch is used to tie a rope around a pole (see Fig. 9). It is part of a granny knot and therefore its transfer function is given by

$$T_{ch} = e^{-\mu_p \Phi_p - \mu \Phi} \frac{1 - 2\mu e^{\frac{1}{2}(\mu_p \Phi_p + \mu \Phi)}}{1 + 2\mu e^{-\frac{1}{2}(\mu_p \Phi_p + \mu \Phi)}}. \quad (22)$$

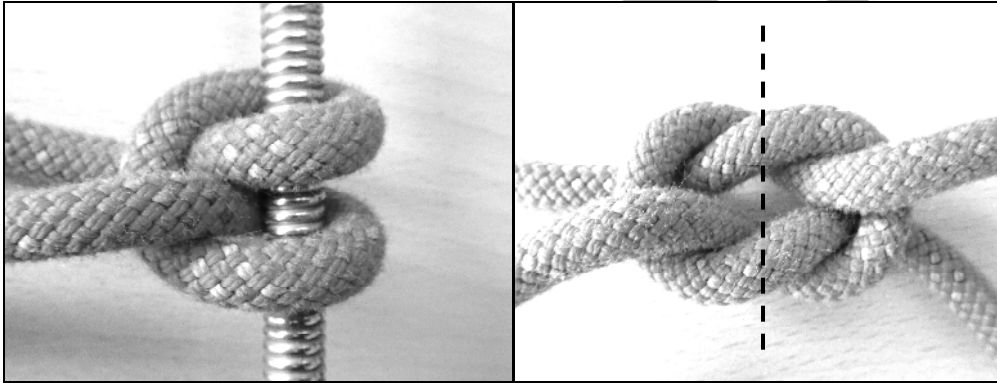


Fig. 9ab. Picture (9a) of the clove hitch in comparison with the granny knot (9b).

One has to distinguish between two different contacts with two friction coefficients μ_p and μ between rope/pole and rope/rope. The contact angle with the pole is $\Phi_p \cong 2\pi$ and the contact angle Φ between the different rope parts is half of the granny knot (see Ref. [13] for a more accurate estimation of Φ and Φ_p). For the same friction coefficients $\mu_p = \mu$, its stability is approximately equal to that of the square knot.

The munter hitch, sometimes called half clove hitch, is an unstable knot because there are no sandwiched rope segments. It is approximately given by the first term of T_{ch}

$$T_{mh} \approx e^{-\mu_p \Phi_p - \mu \Phi}. \quad (23)$$

5. The Zeppelin knot

The Zeppelin knot is a symmetric, but complicated looking knot with some new features. There are three compressing normal forces which lead to a very stable knot.

The determination of the contact angles is simple because the knot has essentially full or half turns of its strands.

Applying the procedure of section 3, the following equations are obtained

$$e^{\mu\gamma}(F_1 + \mu N_1) = F_0 \quad (24)$$

$$F_2 = F_1 e^{-\mu\pi} - \mu N_1 e^{-\frac{\mu\pi}{2}} \quad (25)$$

$$F_3 = F_2 e^{-\mu\pi} . \quad (26)$$

Eq. (24) describes the forces on the rope segment $\overline{01}$ called A (Fig. 10a). For impending motion, its direction equals the direction of segment B. Therefore the friction contribution due to the compression force N_1 is only counted once. There is a small contact angle γ shown in Figure 10b. Eq. (25) follows the same reasoning. The contact angle of the segment $\overline{23}$ is given by π , which leads to Eq. (26).

The equation which is mainly responsible for the high stability of the Zeppelin knot is given by

$$F_4 = F_3 e^{-\frac{\mu\pi}{2}} - 2\mu N_2 - 2\mu N_3 . \quad (27)$$

The segment $\overline{34}$ is compressed by two force pairs (one is indicated by the arrows in Figure 9b) and the segments $\overline{34}$ of both strands move against each other.

The force F'_3 on A in perpendicular direction is balanced by the opposite force N_1 , thus

$$N_1 = F'_3 = F_3 e^{\frac{\pi}{2}\mu} . \quad (28)$$

F_3 is smaller than F'_3 by an Euler-Eytelwein factor with angle $\pi/2$. The remaining forces N_2 and N_3 are obtained considering the force balance in horizontal direction at C (Fig. 10b) with the result

$$N_2 = N_3 \approx F_1 + F_2 - F_3 . \quad (29)$$

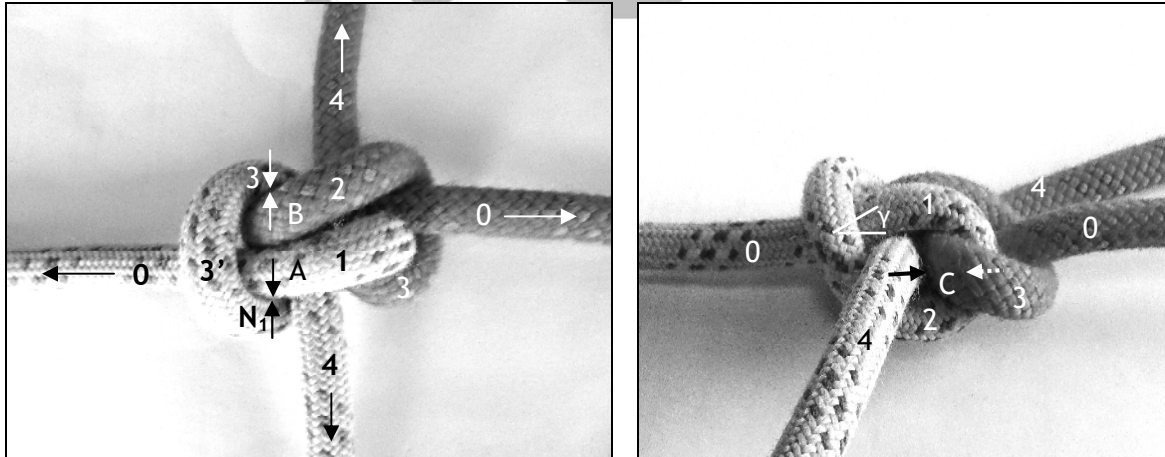


Figure 10ab. The Zeppelin knot viewed from above (10a) and from the side (10b).

From the Eqs. (24) – (29), the transfer function can be calculated with the result

$$T = \frac{F_4}{F_0} = e^{-\mu\Phi} \frac{1 - 4\mu e^{\frac{\mu\pi}{2}} (1 + \mu + e^{\mu\pi} - e^{-\mu\pi})}{1 + \mu e^{-\mu\pi} + \mu e^{-\frac{3\pi}{2}\mu}} . \quad (30)$$

Because γ is small, the contact angle can be approximated to $\Phi = \frac{5}{2}\pi + \gamma \approx \frac{5}{2}\pi$.

6. Comparison with experiments and summary

In the following table, the results of the previous sections are summarized.

knot	M	Φ	μ_c	$1/T(\mu = 0.08)$	measured $1/T$
grief knot Eq. (21)	2	$1.35\pi - 1.75\pi$	unstable	1.55 – 1.71	1.0 ± 0.6
theft knot Eq. (21)	2	$2.35\pi - 2.75\pi$	unstable	1.99 – 2.21	2.15 ± 0.5
granny knot Eq.(19)	4	$1.6\pi - 2\pi$	0.24 – 0.26	2.10 – 2.34	2.5 ± 1.1
square knot Eq.(19)	4	$2.6\pi - 3\pi$	0.20 – 0.21	2.68 – 3.08	2.9 ± 0.5
Zeppelin knot Eq.(30)	6	$\approx 2.5\pi$	0.094	8.08	9.4 ± 1.5
Clove knot Eq. (22)	4	2.75π	0.2	3.08	
Munter hitch Eq. (23)	0	2.75π	unstable	2.00	
Bowline [14]	2	1.5π	0.36		

Table 1. Summary of the properties of the discussed knots. M is the contact number which counts the compressed knot segments by the simultaneous contact of three rope segments. The contact angles Φ of the grief and theft knot are smaller by about $2\eta \approx \pi/4$, because these knots are sheared by the external torque which reduces Φ . The coefficient of friction for Dyneema fibres was assumed as 0.08.

The experimentally determined friction coefficients by Crowell [7] that lead either to self-locking or slipping agree with the theoretical results from table (1), column 4.

The published experimental pulling forces for a given hold force by Patil et al. [7] are found in column 6. The theoretical results of column 5 can explain these measurements.

Because of its practical importance, the difference between the glove and munter hitch has to be mentioned. The stability of the glove hitch is used by climbers and mountaineers. With the help of this knot, a safe belay is obtained without any rope slip under load. On the contrary, it is desirable that the munter hitch slips when a heavy fall occurs in order to control this fall. Experimentally, for a hand force of about 400 N, the rope begins to slip at about 3000 N, that is $T_{mh} \approx 0.13$ which is in agreement with Eq. (23) assuming reasonable friction coefficients for nylon ropes. This is an indication that the simple model of dry friction with only one parameter, the friction coefficient μ , is a sufficiently good approximation for the description of the friction inside a knot.

Examination of the transfer functions of table (1) reveals the following general properties. First, although there are many angle variables in the force balance equations during the calculation, these angles often finally add and enter as a total in the contact angle Φ . Because of its few parameters and its transparency, the validity of the model can be easily checked. Second, Taylor expansion for small μ yields

$$T(\mu, \Phi) \rightarrow 1 - (M + \Phi)\mu.$$

In this limit, T is determined only by two parameters, the (triple) contact number M and the contact angle Φ .

M is twice the number of sandwiched segments which are compressed by opposing force pairs from surrounding knot segments and which move against each other. If the sandwiched segments move in the same direction, they are counted as one segment.

For example, for the Square knot, the compression forces N (see Fig. 3), the segments $\overline{12}$ and $\overline{23}$ press on the two segments $\overline{3'4'}$ and $\overline{0'1'}$ which move in different directions, which

gives a total of $M = 4$. In the directed graph representation (see Fig. 6), M corresponds to the additional number of arrows (besides those of the trivial forward path) which point to a node. For the stability of a knot, M has to be greater than zero. Its size strongly influences the holding force of a knot and is therefore very useful to characterize it. A similar number counting the crossings in the knot has been used to classify of a knot [7]. The crossing point number, however, is related to the knot length [15, 16], and is already included in the contact angle Φ . Φ contains the entire double contacts of the knot segments. Triple contacts are considered by the number M , so that the entire frictional contact inside a knot has been taken into account. Thus, a complete description of the holding force and the stability of a knot for a perfectly flexible and inextensible rope with dry friction has been achieved.

¹ C. Adams, *The Knot Book: An Elementary Introduction to the Mathematical Theory of Knots* (American Mathematical Society, ISBN 978-0-8218-3678-1, 2004)

² L.H. Kauffman, *Series on Knots and Everything*. <https://webeducation.com/wp-content/uploads> (2019)

³ M. Gommers, <http://www.paci.com.au/knots.php>

⁴ B. Bayman, Theory of hitches. *Am. J. Phys.*, 45, 185 (1977)

⁵ J.H. Maddocks, J.B. Keller, Ropes in Equilibrium. *SIAM J Appl. Math.* 47 (1987)

⁶ B. Crowell, The physics of knots. www.lightandmatter.com

⁷ V.P. Patil, J.D. Sandt, M. Kolle, J. Dunkel, Topological Mechanics of Knots and Tangles. *Science* 367 (6473) (2020)

⁸ V. A. Lubarda, The mechanics of belt friction revisited. *International Journal of Mechanical Engineering Education*, Volume 42, Number 2 (2014)

⁹ T. Shifrin, *Differential Geometry: A First Course in Curves and Surfaces* (2013)

¹⁰ S.J. Mason, Feedback Theory - Further Properties of Signal Flow Graph (PDF). *Proceedings of the IRE.* 44 (7) (1956)

¹¹ P. Pieranski, S. Przybyl, A. Stasiak. Tight open knots, *Eur. Phys. J. E* 6, 123-128 (2001)

¹² P. Johanns, P. Grandgeorge, C. Baek, T. Sano, J. Maddocks, P. Reis, The shapes of physical trefoil knots. *Extreme Mechanics Letters* 43 (2021) 101172

¹³ F. Fuss, G. Niegl, Understanding the mechanics of dynamic rope brakes. <https://www.sciencedirect.com/science/article/pii/S1877705810004066> (2010)

¹⁴ to be published at sigmadewe.com

¹⁵ J. Cantarella, R.B. Kusner, J.M. Sullivan, On the minimum ropelength of knots and links (PDF), *Inventiones Mathematicae*, 150 (2) (2002)

¹⁶ Y. Diao, C. Ernst, A. Por, U. Ziegler, *Journal of Knot Theory and its Ramifications*, 28 (14) (2019)